

AD-A122 069

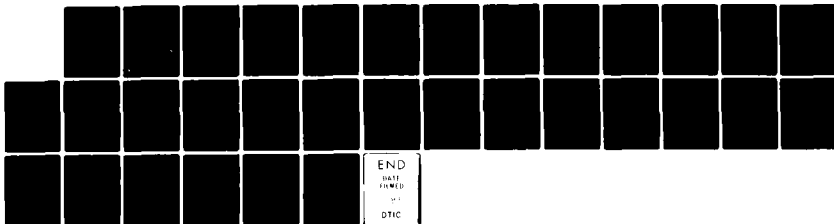
RIPRAP STABILITY SCALE EFFECTS(U) COASTAL ENGINEERING  
RESEARCH CENTER FORT BELVOIR VA L L BRODERICK ET AL  
AUG 82 CERC-TP-82-3

1/1

UNCLASSIFIED

F/G 12-2

NI





MICROCOPY RESOLUTION TEST CHART  
NATIONAL BUREAU OF STANDARDS-1963-A

AD A 122 069

CIRK TP 82-3

(12)

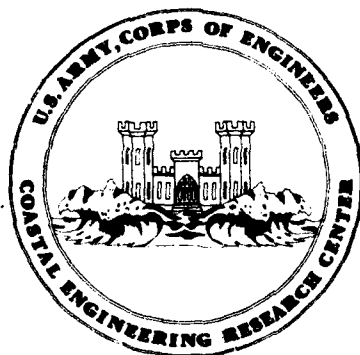
# Riprap Stability Scale Effects

by

Laurie L. Broderick and John P. Ahrens

TECHNICAL PAPER NO. 82-3

AUGUST 1982



Approved for public release;  
distribution unlimited.

DTIC  
ELECTE  
DEC 6 1982

A

U.S. ARMY, CORPS OF ENGINEERS  
COASTAL ENGINEERING  
RESEARCH CENTER

Kingman Building  
Fort Belvoir, Va. 22060

82 12 06 015

DTIC FILE COPY

Reprint or republication of any of this material shall give appropriate credit to the U.S. Army Coastal Engineering Research Center.

Limited free distribution within the United States of single copies of this publication has been made by this Center. Additional copies are available from:

*National Technical Information Service  
ATTN: Operations Division  
5285 Port Royal Road  
Springfield, Virginia 22161*

The findings in this report are not to be construed as an official Department of the Army position unless so designated by other authorized documents.

UNCLASSIFIED

SECURITY CLASSIFICATION OF THIS PAGE (When Data Entered)

REPORT DOCUMENTATION PAGE		READ INSTRUCTIONS BEFORE COMPLETING FORM
1. REPORT NUMBER TP 82-3	2. GOVT ACCESSION NO. AD-A122069	3. RECIPIENT'S CATALOG NUMBER
4. TITLE (and Subtitle)  RIPRAP STABILITY SCALE EFFECTS		5. TYPE OF REPORT & PERIOD COVERED Technical Report
		6. PERFORMING ORG. REPORT NUMBER
7. AUTHOR(s) Laurie L. Broderick John P. Ahrens		8. CONTRACT OR GRANT NUMBER(s)
9. PERFORMING ORGANIZATION NAME AND ADDRESS Department of the Army Coastal Engineering Research Center (CERRE-CS) Fort Belvoir, Virginia 22060		10. PROGRAM ELEMENT, PROJECT, TASK AREA & WORK UNIT NUMBERS  D31680
11. CONTROLLING OFFICE NAME AND ADDRESS Department of the Army Coastal Engineering Research Center Kingman Building, Fort Belvoir, Virginia 22060		12. REPORT DATE August 1982
		13. NUMBER OF PAGES 29
14. MONITORING AGENCY NAME & ADDRESS (if different from Controlling Office)		15. SECURITY CLASS. (of this report)  UNCLASSIFIED
		15a. DECLASSIFICATION/DOWNGRADING SCHEDULE
16. DISTRIBUTION STATEMENT (of this Report)  Approved for public release; distribution unlimited.		
17. DISTRIBUTION STATEMENT (of the abstract entered in Block 20, if different from Report)		
18. SUPPLEMENTARY NOTES		
19. KEY WORDS (Continue on reverse side if necessary and identify by block number)  <div style="display: flex; justify-content: space-between;"> <div>Riprap stability Small scale Prototype scale</div> <div>Waves Scale effects</div> </div>		
20. ABSTRACT (Continue on reverse side if necessary and identify by block number) <p>This report is based on small-scale tests of riprap stability at a 1:10 (model:prototype) Froude scale, which replicate previous tests conducted in the large wave tank at the Coastal Engineering Research Center (CERC). The large wave tank tests used wave heights which exceeded 5 feet in some instances and can be regarded as prototype scale. Scale effects were approximately 20 percent at the zero-damage level, and the small-scale tests gave more conservative estimates of zero-damage wave heights and wave runups than those</p> <p style="text-align: right;">(continued)</p>		

DD FORM 1 JAN 73 1473

EDITION OF 1 NOV 65 IS OBSOLETE

UNCLASSIFIED

SECURITY CLASSIFICATION OF THIS PAGE (When Data Entered)

Cont'd

UNCLASSIFIED

SECURITY CLASSIFICATION OF THIS PAGE(When Data Entered)

predicted from prototype test values. However, for severe levels of damage the differences between small scale and prototype were not as great. When profile surveys of severely damaged riprap were compared, the small-scale and the prototype profiles were found to have similar shapes. Wave period was also found to have less influence on the zero-damage wave heights in the small-scale tests than in the prototype tests. The results of these tests were compared with studies conducted by Dai and Kamel (1969), Thomsen, Wohlt, and Harrison (1972), and the Hydraulic Research Station (1975).

UNCLASSIFIED

SECURITY CLASSIFICATION OF THIS PAGE(When Data Entered)

## PREFACE

This report is published to provide engineers an evaluation of riprap stability in monochromatic waves, tested at small scale. The results will also be used to evaluate future small-scale tests of riprap stability under irregular wave attack. The work was carried out under the U.S. Army Coastal Engineering Research Center's (CERC) Riprap Stability to Irregular Wave Attack work unit, Coastal Structure Evaluation and Design Program, Coastal Engineering Area of Civil Works Research and Development.

The report was prepared by Laurie L. Broderick, Hydraulic Engineer, and John P. Ahrens, Oceanographer, under the supervision of Dr. R.M. Sorensen, Chief, Coastal Processes and Structures Branch, and Mr. R.P. Savage, Chief, Research Division.

Technical Director of CERC was Dr. Robert W. Whalin, P.E., upon publication of this report.

Comments on this publication are invited.

Approved for publication in accordance with Public Law 166, 79th Congress, approved 31 July 1945, as supplemented by Public Law 172, 88th Congress, approved 7 November 1963.

*Ted E. Bishop*  
TED E. BISHOP  
Colonel, Corps of Engineers  
Commander and Director



Accession For

WHS GRAB ☒

1911-12 ☐

1912-13 ☐

1913-14 ☐

1914-15 ☐

1915-16 ☐

1916-17 ☐

1917-18 ☐

1918-19 ☐

1919-20 ☐

1920-21 ☐

1921-22 ☐

1922-23 ☐

1923-24 ☐

1924-25 ☐

1925-26 ☐

1926-27 ☐

1927-28 ☐

1928-29 ☐

1929-30 ☐

1930-31 ☐

1931-32 ☐

1932-33 ☐

1933-34 ☐

1934-35 ☐

1935-36 ☐

1936-37 ☐

1937-38 ☐

1938-39 ☐

1939-40 ☐

1940-41 ☐

1941-42 ☐

1942-43 ☐

1943-44 ☐

1944-45 ☐

1945-46 ☐

1946-47 ☐

1947-48 ☐

1948-49 ☐

1949-50 ☐

1950-51 ☐

1951-52 ☐

1952-53 ☐

1953-54 ☐

1954-55 ☐

1955-56 ☐

1956-57 ☐

1957-58 ☐

1958-59 ☐

1959-60 ☐

1960-61 ☐

1961-62 ☐

1962-63 ☐

1963-64 ☐

1964-65 ☐

1965-66 ☐

1966-67 ☐

1967-68 ☐

1968-69 ☐

1969-70 ☐

1970-71 ☐

1971-72 ☐

1972-73 ☐

1973-74 ☐

1974-75 ☐

1975-76 ☐

1976-77 ☐

1977-78 ☐

1978-79 ☐

1979-80 ☐

1980-81 ☐

1981-82 ☐

1982-83 ☐

1983-84 ☐

1984-85 ☐

1985-86 ☐

1986-87 ☐

1987-88 ☐

1988-89 ☐

1989-90 ☐

1990-91 ☐

1991-92 ☐

1992-93 ☐

1993-94 ☐

1994-95 ☐

1995-96 ☐

1996-97 ☐

1997-98 ☐

1998-99 ☐

1999-00 ☐

2000-01 ☐

2001-02 ☐

2002-03 ☐

2003-04 ☐

2004-05 ☐

2005-06 ☐

2006-07 ☐

2007-08 ☐

2008-09 ☐

2009-10 ☐

2010-11 ☐

2011-12 ☐

2012-13 ☐

2013-14 ☐

2014-15 ☐

2015-16 ☐

2016-17 ☐

2017-18 ☐

2018-19 ☐

2019-20 ☐

2020-21 ☐

2021-22 ☐

2022-23 ☐

2023-24 ☐

2024-25 ☐

2025-26 ☐

2026-27 ☐

2027-28 ☐

2028-29 ☐

2029-30 ☐

2030-31 ☐

2031-32 ☐

2032-33 ☐

2033-34 ☐

2034-35 ☐

2035-36 ☐

2036-37 ☐

2037-38 ☐

2038-39 ☐

2039-40 ☐

2040-41 ☐

2041-42 ☐

2042-43 ☐

2043-44 ☐

2044-45 ☐

2045-46 ☐

2046-47 ☐

2047-48 ☐

2048-49 ☐

2049-50 ☐

2050-51 ☐

2051-52 ☐

2052-53 ☐

2053-54 ☐

2054-55 ☐

2055-56 ☐

2056-57 ☐

2057-58 ☐

2058-59 ☐

2059-60 ☐

2060-61 ☐

2061-62 ☐

2062-63 ☐

2063-64 ☐

2064-65 ☐

2065-66 ☐

2066-67 ☐

2067-68 ☐

2068-69 ☐

2069-70 ☐

2070-71 ☐

2071-72 ☐

2072-73 ☐

2073-74 ☐

2074-75 ☐

2075-76 ☐

2076-77 ☐

2077-78 ☐

2078-79 ☐

2079-80 ☐

2080-81 ☐

2081-82 ☐

2082-83 ☐

2083-84 ☐

2084-85 ☐

2085-86 ☐

2086-87 ☐

2087-88 ☐

2088-89 ☐

2089-90 ☐

2090-91 ☐

2091-92 ☐

2092-93 ☐

2093-94 ☐

2094-95 ☐

2095-96 ☐

2096-97 ☐

2097-98 ☐

2098-99 ☐

2099-00 ☐

2100-01 ☐

2101-02 ☐

2102-03 ☐

2103-04 ☐

2104-05 ☐

2105-06 ☐

2106-07 ☐

2107-08 ☐

2108-09 ☐

2109-10 ☐

2110-11 ☐

2111-12 ☐

2112-13 ☐

2113-14 ☐

2114-15 ☐

2115-16 ☐

2116-17 ☐

2117-18 ☐

2118-19 ☐

2119-20 ☐

2120-21 ☐

2121-22 ☐

2122-23 ☐

2123-24 ☐

2124-25 ☐

2125-26 ☐

2126-27 ☐

2127-28 ☐

2128-29 ☐

2129-30 ☐

2130-31 ☐

2131-32 ☐

2132-33 ☐

2133-34 ☐

2134-35 ☐

2135-36 ☐

2136-37 ☐

2137-38 ☐

2138-39 ☐

2139-40 ☐

2140-41 ☐

2141-42 ☐

2142-43 ☐

2143-44 ☐

2144-45 ☐

2145-46 ☐

2146-47 ☐

2147-48 ☐

2148-49 ☐

2149-50 ☐

2150-51

## CONTENTS

	Page
CONVERSION FACTORS, U.S. CUSTOMARY TO METRIC (SI) . . . . .	6
SYMBOLS AND DEFINITIONS . . . . .	7
I INTRODUCTION . . . . .	9
II TEST SETUP AND PROCEDURE . . . . .	9
1. Large Wave Tank (LWT) Tests . . . . .	9
2. Small-Scale Tests . . . . .	10
III METHOD OF DATA ANALYSIS . . . . .	14
IV COMPARISON OF MODEL AND PROTOTYPE DATA . . . . .	16
1. Damage . . . . .	16
2. Profile Shapes . . . . .	19
3. Runup . . . . .	21
4. Flow Regime . . . . .	21
V COMPARISON WITH OTHER SOURCES OF DATA . . . . .	23
VI RESULTS AND CONCLUSIONS . . . . .	27
LITERATURE CITED . . . . .	29

## TABLES

1 Basic Data . . . . .	17
2 Correlation coefficients for model and prototype profiles . . . . .	22
3 Runup . . . . .	22
4 Flow regime computations . . . . .	24
5 HRS data . . . . .	26

## FIGURES

1 Profile view of wave tank and test setup . . . . .	11
2 Armor gradation analysis . . . . .	12
3 Filter gradation analysis . . . . .	12
4 Riprap damage profile . . . . .	15
5 Typical small-scale and prototype damage trends for $d/gT^2 = 0.0144$ . . . . .	15
6 Zero-damage stability numbers, damage rate coefficients, and relative runup versus relative depth . . . . .	18



## CONTENTS

### FIGURES—Continued

	Page
7 Small-scale and prototype damage trends for $d/gT^2 = 0.0144$ . . . . .	19
8 Small-scale and prototype damage profile comparison for $dgT^2 = 0.0264$ . . . . .	20
9 Small-scale and prototype damage profile comparison for $d/gT^2 = 0.0037$ . . . . .	20
10 Flow regime . . . . .	25
11 Scale effects factor versus Reynolds number for various sources of data . . . . .	25
12 Stability numbers versus Reynolds numbers, HRS data . . . . .	28

# CONVERSION FACTORS, U.S. CUSTOMARY TO METRIC (SI) UNITS OF MEASUREMENT

U.S. customary units of measurement used in this report can be converted to metric (SI) units as follows:

Multiply	by	To obtain
inches	25.4	millimeters
	2.54	centimeters
square inches	6.452	square centimeters
cubic inches	16.39	cubic centimeters
feet	30.48	centimeters
	0.3048	meters
square feet	0.0929	square meters
cubic feet	0.0283	cubic meters
yards	0.9144	meters
square yards	0.836	square meters
cubic yards	0.7646	cubic meters
miles	1.6093	kilometers
square miles	259.0	hectares
knots	1.852	kilometers per hour
acres	0.4047	hectares
foot-pounds	1.3558	newton meters
millibars	$1.0197 \times 10^{-3}$	kilograms per square centimeter
ounces	28.35	grams
pounds	453.6	grams
	0.4536	kilograms
ton, long	1.0160	metric tons
ton, short	0.9072	metric tons
degrees (angle)	0.01745	radians
Fahrenheit degrees	5/9	Celsius degrees or Kelvins <sup>1</sup>

<sup>1</sup>To obtain Celsius (C) temperature readings from Fahrenheit (F) readings, use formula:  $C = (5/9) (F - 32)$ .

To obtain Kelvin (K) readings, use formula:  $K = (5/9) (F - 32) + 273.15$ .

## SYMBOLS AND DEFINITIONS

$a_{im}/k$	roughness term
$C_g$	group velocity (meters per second)
$D$	damage to the profile (cubic centimeters)
$D'$	dimensionless damage
$d$	water depth in flat part of tank (centimeters)
$d_{15}$	equivalent diameter of the riprap stone; 15 percent of the total weight of the armor gradation is contributed by stones of lesser weight (millimeters)
$d_{85}$	equivalent diameter of the filter stone; 85 percent of the total weight of the filter gradation is contributed by stones of lesser weight (millimeters)
$g$	acceleration due to gravity (9.81 meters per second)
$H$	incident wave height (centimeters)
$H_z$	wave height at the zero-damage level (centimeters)
$L$	wavelength (centimeters)
$L_o$	deepwater wavelength (feet)
$N_s$	stability number
$N_z$	stability number at the zero-damage level
$\bar{N}_{zp}$	stability number at the zero-damage level divided by the average of the prototype stability numbers at the zero-damage level
$Re$	Reynolds number with roughness term
$R_N$	Reynolds number using wave height
$R_z$	runup at the zero-damage level
$S$	distance from wave blade to toe of embankment (meters)
$T$	wave period (seconds)
$W_d$	wave burst duration (seconds)
$W_{50}$	median armor stone weight (kilograms); weight of stone where 50 percent of the total weight of the armor gradation is contributed by stones of lesser weight

# SYMBOLS AND DEFINITIONS--Continued

$w_r$	unit weight of riprap; 2707.1 kilograms per cubic meter in this study
$w_w$	unit weight of water; 1000 kilograms per cubic meter
$\xi$	surf parameter (centimeters squared per second)
$\theta$	angle formed between embankment slope and horizontal
$\nu$	kinematic viscosity

## RIPRAP STABILITY SCALE EFFECTS

by  
*Laurie L. Broderick and John P. Ahrens*

### I. INTRODUCTION

Small-scale wave tank tests of riprap stability were conducted at the U.S. Army Coastal Engineering Research Center (CERC), and the results were compared with previously conducted large-scale tests of riprap stability (Ahrens, 1975) to determine the nature and magnitude of scale effects. The large-scale tests, conducted in CERC's large wave tank (LWT), used wave heights which exceeded 1.5 meters in some instances and can be regarded as prototype scale. The small-scale tests replicated the LWT tests at a 1:10 (model:prototype) Froude scale. Both small-scale and LWT tests were conducted using monochromatic waves (waves of constant height and period). The results of the experiments were used to evaluate scale effects correction factors. These results will also be used to evaluate future small-scale tests of riprap stability using irregular waves, the next phase in this study.

It has only been in the last few years that irregular wave conditions could be satisfactorily generated in the laboratory but only at small scales, because of the unavailability of a prototype-scale irregular wave research facility. This investigation of scale effects will allow, with some confidence, the extrapolation of the small-scale test results to prototype scale when the model/prototype-scale ratio is 1:10. It will also give general insight into the nature of scale effects to be expected when conducting model experiments at other scale ratios.

### II. TEST SETUP AND PROCEDURE

#### 1. Large Wave Tank (LWT) Tests.

Ahrens' (1975) large-scale tests were conducted in the LWT which is 193.6 meters long, 4.6 meters wide, and 6.10 meters deep. A stillwater depth of 4.6 meters was used for all tests. The distance between the toe of the embankment and the mean position of the wave generator blade varied from about 119 to 137 meters, depending on the slope of the embankment being tested. Details on the wave tank and generator are given in Coastal Engineering Research Center (1980).

The embankment was made up of core material, a filter layer, and an armor layer. The core material was compacted bank-run gravel, graded to the desired slope, and was essentially impermeable to wave penetration. The filter layer, 15 to 21 centimeters thick, was placed between the core material and the armor layer. The filter stone was sized such that the ratio of the 15 percent finer diameter of the riprap stone,  $d_{15}$ , to the 85 percent finer diameter of the filter stone,  $d_{85}$ , was usually less than 4 and always less than 5. The armor stone, which was a diorite with a specific gravity of 2.71, was divided into three stockpiles according to the median weight,  $W_{50}$ . One stockpile ranged from 12.2 to 16.3 kilograms, another from 33.1 to 35.4 kilograms, and the third was constant at 54.4 kilograms. The relative size gradations of the three stockpiles were the same; the specified maximum stone weight was four times the median weight and the minimum weight was one-eighth of the median weight.

In the LWT tests the following parameters were varied systematically: wave height, embankment slope, riprap weight, and wave period. Wave heights varied from 0.43 to 1.83 meters; wave periods ranged from 2.8 to 11.3 seconds; the embankment slopes tested were 1 on 2.5, 1 on 3.5, and 1 on 5; and the median riprap weight varied from 12.2 to 54.4 kilograms.

## 2. Small-Scale Tests.

The small-scale tests were run in one of CERC's small wave tanks, 0.46 meter wide by 0.91 meter deep by 45.7 meters long, which was used to replicate the LWT at a 1:10 Froude scale. The width of the small tank is one-tenth of the LWT, and the distance from the toe of the embankment to the mean position of the blade was made one-tenth of the distance in the LWT. Figure 1 shows a profile view of the tank used in the small-scale tests.

In the small-scale tests the wave height and wave period were varied, but the embankment slope and median riprap weight were fixed. The embankment slope for the small-scale tests was 1 on 3.5 which was one of the slopes tested in the LWT. The median riprap weight was fixed at 0.034 kilogram which replicates the stockpile of riprap with a median riprap weight of 34 kilograms used in the LWT when scaled down using the Froude scale.

The riprap armor layer in the small-scale tests was the same material and from the same quarry as that used in the prototype tests, diorite with a specific gravity of 2.71. The gradation of the model armor ranged in weight from four times to one-eighth the median weight of 0.034 kilogram, the same gradation as that used in the prototype (Fig. 2). A gradation analysis was run both before and after testing to determine if the gradation of the armor unit changed over time. As shown in Figure 2, the two gradations appear to be about the same.

The filter layer consisted of small gravel with a 3- to 8-millimeter diameter and was constructed to approximately one-tenth prototype scale; model and prototype filter layer gradations are shown in Figure 3.

The core material was compacted sand with a median diameter of 0.2 millimeter. No attempt was made to replicate the core material at a 1:10 Froude scale which is effectively impermeable in both model and prototype.

Waves were run in bursts of short duration with an interval of about 1 minute between bursts to allow the wave energy in the tank to dampen out. The duration of the wave burst was set equal to

$$W_d = \frac{2S}{C_g} \quad (1)$$

where  $W_d$  is the wave burst duration,  $S$  the distance from wave blade to toe of embankment, and  $C_g$  the group velocity of the waves. The number of wave bursts run at a particular wave height in the model, which was equal to the number of wave bursts in the prototype, was normally enough to ensure that the riprap profile was at equilibrium for the given wave height and period. The minimum number of waves run at a particular wave height ranged from 340 for the longest period waves to 1,050 for the shortest period waves. After the required number of waves had been generated, the condition of riprap surface

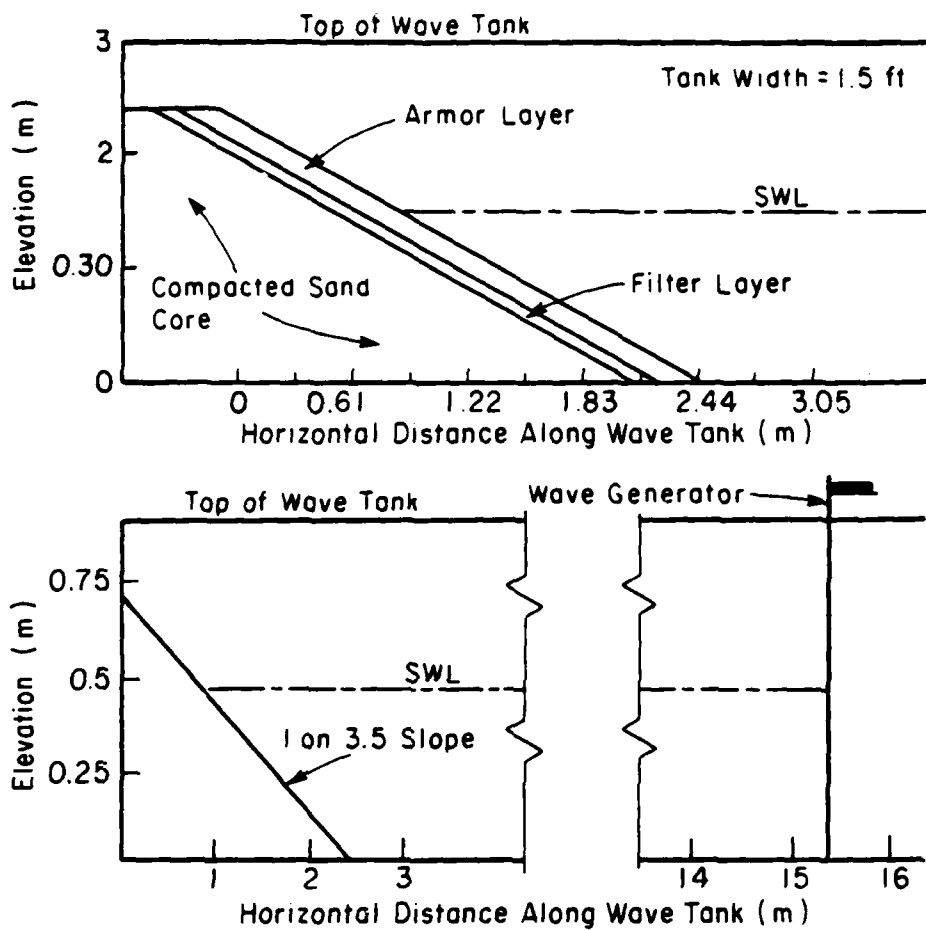


Figure 1. Profile view of wave tank and test setup.

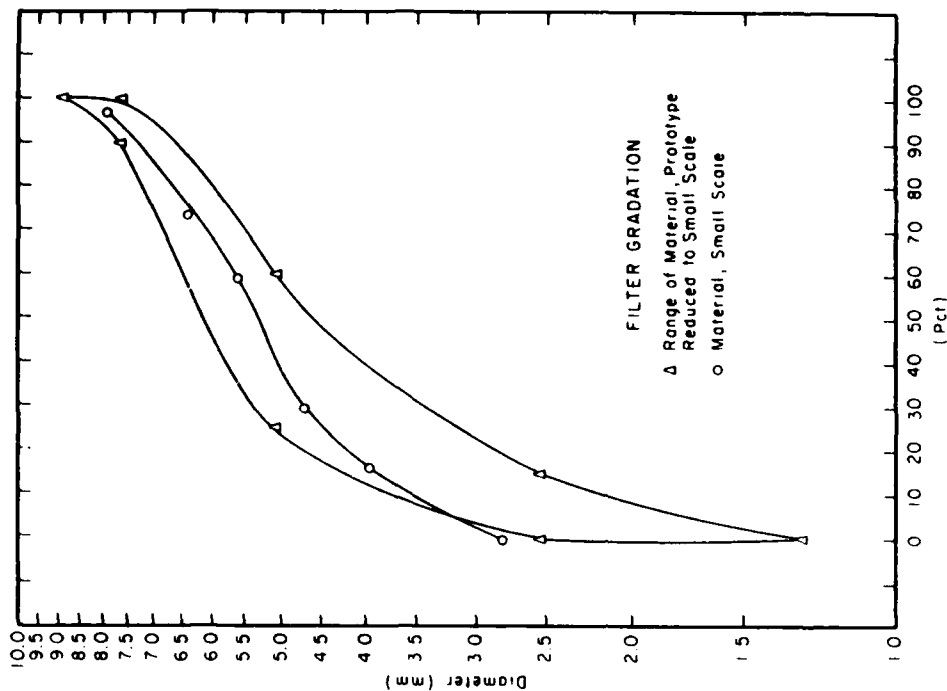


Figure 3. Filter gradation analysis.

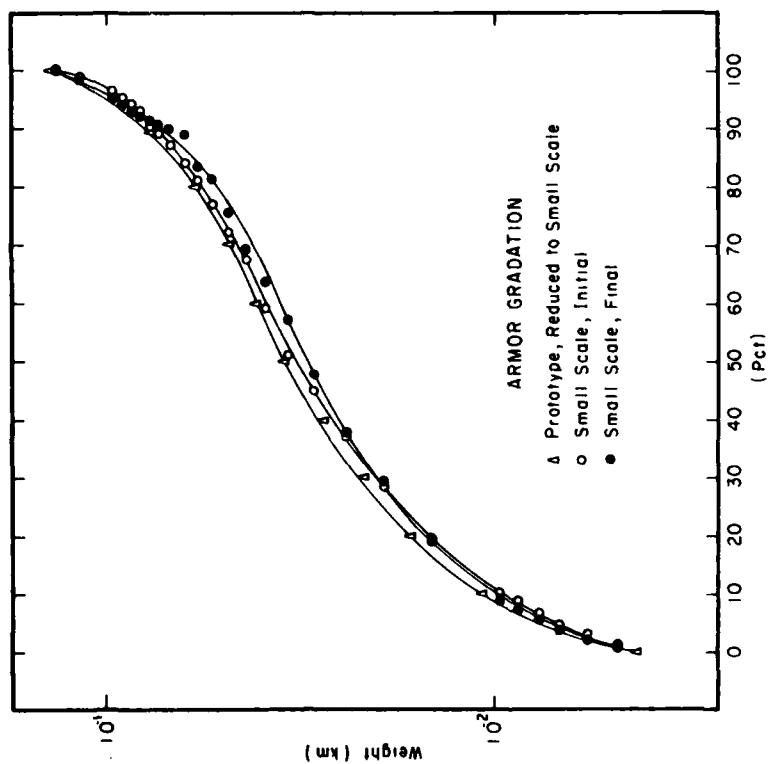


Figure 2. Armor gradation analysis.



was documented; the wave height was then increased approximately 10 percent, and wave bursts were generated again. This procedure was continued until a wave height was reached which caused failure of the riprap. Failure was defined as the riprap being shifted enough to expose part of the filter layer which was removed by the wave action.

The incident wave height was calculated using strip-chart recordings from two resistance-type wave gages spaced one-quarter of a wavelength apart and placed as close to the wave generator as feasible such that the waveform stabilizes. The gages were placed as close to the blade as convenient to increase the recording time of the gages before the waves were reflected from the structure and returned to the gages. The average wave height, which was the average of the wave heights for each gage, was measured by visual inspection of the strip-chart recordings.

In the LWT tests, a correction was applied to the wave height because of the last wave effect (Madsen, 1970). The term "last wave effect" refers to the occurrence of one to three waves noticeably higher than the modal wave height; the number of higher waves is related to the water depth-to-wavelength ratio,  $d/L$ . This term was used because the highest wave usually occurred near the end of the burst. A high wave also occurred near the beginning of the burst, causing the highest waves to bracket the smaller waves of almost uniform height. These smaller waves were considered the modal waves.

The highest waves in the burst caused more stone movement than the modal waves; thus, a correction was made to the modal wave height. The use of the modal wave height to characterize the height of a wave burst would result in an invalid comparison of riprap stability for tests with different wave periods. The correction to the modal wave height was determined by the depth-to-wavelength ratio,  $d/L$ : a decrease from 1.11 for a wave period of 2.8 seconds to 1.04 for a wave period of 11.3 seconds.

The last wave effect was not apparent in the small-scale tests because of the initial and final position of the wave generator blade. The initial and final position of the blade in the LWT tests was in the center of its total stroke where the water particle velocities were at a maximum, creating some irregularities in the initial and final waves. In the small-scale tests the blade started and stopped in a rear position where the water particle velocities were zero, causing no apparent irregularities in the wave burst.

The apparatus used to survey the filter layer and riprap armor layer consisted of six vertical sounding rods mounted on a rack that moved along rails mounted on the tank walls. Attached to the end of each survey rod by a ball and socket joint was a foot measuring 1.8 centimeters in diameter which was approximately one-tenth of that used in the LWT tests. The model surface was surveyed in the same manner as that of the prototype. Surface elevations were measured over square grid points 61 by 61 centimeters (prototype, one-tenth of that for the model) apart on a horizontal plane.

The following procedure for the small-scale tests was the same as for the prototype tests (Ahrens, 1975):

- (a) Place and compact core material.
- (b) Place and smooth filter layer material.

- (c) Survey filter layer surface.
- (d) Place riprap armor stone by dumping from a hand-held can to simulate the prototype procedure of dumping from a skip.
- (e) Survey riprap armor layer surface (reference survey).
- (f) During the generation of the predetermined number of wave bursts, collect wave data and visually observe the behavior of the riprap and wave runoff on the riprap surface.
- (g) Survey riprap armor layer.
- (h) Increase wave height approximately 10 percent.
- (i) Repeat steps f, g, and h until failure.
- (j) Conduct final riprap survey.

### III. METHOD OF DATA ANALYSIS

Damage to the riprap armor layer was quantified by comparing the profile of the riprap armor layer taken at some wave height (damage profile) with the profile taken before any waves had attacked the riprap armor (reference profile). The comparison is shown schematically in Figure 4. The change in the reference profile typically consisted of an erosion zone and an accretion zone, as shown in Figure 4. The volume per unit length of the erosion zone was used to quantify the extent of damage to the riprap,  $D$ . Using the median stone weight,  $W_{50}$ , to characterize the size of the riprap, the dimensionless damage,  $D'$ , is given by

$$D' = \frac{D}{\left(\frac{W_{50}}{w_r}\right)^{2/3}} \quad (2)$$

where  $w_r$  is the unit weight of the riprap stone; i.e.,  $D'$  is the equivalent number of median size stones removed by wave attack per median stone length. The word equivalent is used because  $D'$  includes about 40 percent void spaces.

The incident wave height was made dimensionless through the use of the stability number,  $N_s$ , which was developed in Hudson's (1958) study of the stability of rubble-mound breakwaters. The stability number is given by

$$N_s = \frac{H}{\left(\frac{W_{50}}{w_r}\right)^{1/3} \left(\frac{w_r}{w_w} - 1\right)} \quad (3)$$

where  $H$  is the incident wave height, and  $w_w$  the weight of water. Since freshwater ( $w_w = 1000$  kilograms per cubic meter) and the density of the stone ( $w_r = 2707.1$  kilograms per cubic meter) were the same in both prototype and small-scale tests,  $(w_r/w_w - 1) = 1.71$  for all tests.

Data from one small-scale test (SET-1) and one prototype test (SPL-19) are used in Figure 5 to illustrate typical damage trends observed in this study.

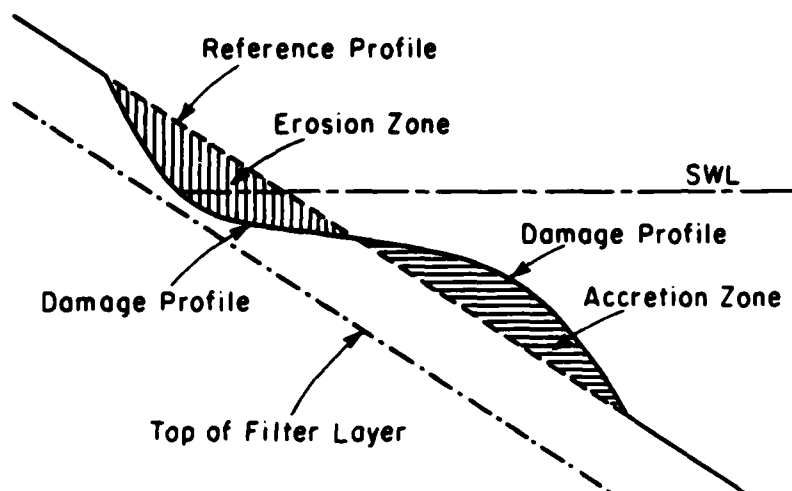


Figure 4. Riprap damage profile.

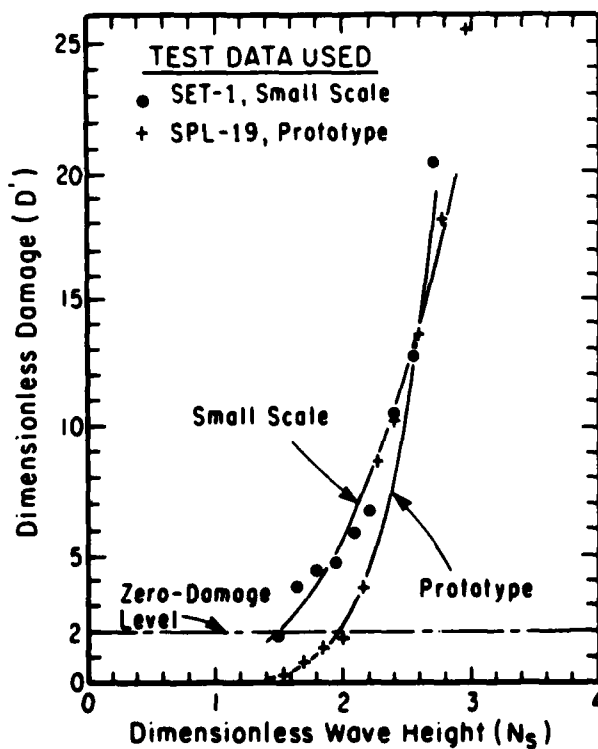


Figure 5. Typical small-scale and prototype damage trends for  $d/gT^2 = 0.0144$ .

The SET-1 test replicated the LWT SPL-19 test at a 1:10 Froude scale. Damage trend refers to the increasing cumulative damage with increasing wave height. Fitted to the data for both tests are curves of the form

$$D' = aN_s^b \quad (4)$$

where  $D'$  is the dimensionless damage,  $N_s$  the dimensionless wave height stability number, and  $a, b$  the dimensionless regression coefficients. Figure 5 shows that the regression curves fit the data well, particularly at low levels of damage, and provide a convenient method of defining the damage trend. Also shown in Figure 5 is the zero-damage level used in this study (i.e.,  $D' = 2.0$ ).  $D' = 2.0$  is about the lowest level of damage that can be consistently detected in the inherent scatter in the survey data.

The two tests in Figure 5 had a relative water depth of  $d/gT^2 = 0.0144$ , where  $d$  is the water depth in the tank,  $T$  the wave period, and  $g$  the acceleration of gravity. In comparing damage trends, both the prototype and small-scale tests were grouped by relative depth (see Table 1) to eliminate the possible influence of wave period effects (Ahrens and McCartney, 1975).

Curves of the form of equation (4) were fitted to the model and prototype data, and the following two parameters were chosen to characterize the damage trend (Table 1): the stability number,  $N_z$ , for  $D' = 2.0$  which characterizes the zero-damage level, and the regression coefficient  $b$  (eq. 4) which characterizes the rate of increase in damage with increasing wave height. The parameters  $N_z$  and  $b$  are tabulated and grouped by relative depth in Table 1 to facilitate comparison of small-scale and prototype values for similar wave conditions.

#### IV. COMPARISON OF MODEL AND PROTOTYPE DATA

##### 1. Damage.

The values of  $N_z$  and  $b$  from Table 1 are plotted versus  $d/gT^2$  in Figure 6 to demonstrate the influence of both the scale effects and the wave period effects on  $N_z$  and  $b$ . The figure shows that the small-scale tests had lower values of  $N_z$  and generally lower values of  $b$  than the prototype tests with similar wave conditions. This finding indicates that damage is initiated earlier in the small-scale tests than in the prototype tests but proceeds at a slower rate, with respect to increased wave height. The convergence in the damage trends typical of small-scale and prototype tests can be seen in Figure 5. The regression curves cross; however, the actual data indicate that while the damage levels in the small-scale tests may approach those of the prototype, they do not surpass them for similar values of the dimensionless wave height. Figure 7 is similar to Figure 5 except it shows all the data for tests where  $d/gT^2 = 0.0144$ , which includes the data in Figure 5. The small-scale and prototype data fields overlap somewhat, but the crossover suggested by the regression curves in Figure 5 does not occur. For the tests where  $d/gT^2 = 0.0264$  and  $0.0065$ , there is more overlap or convergence of small-scale and prototype data fields than shown in Figure 7; for tests where  $d/gT^2 = 0.0037$  there is no overlap and little convergence in the damage trends. The reason for the convergence of damage trends is unclear, but it may reflect the influence of breaker characteristics or may be caused by the size of the data set and the inherent scatter in the data. Convergence in the damage trend indicates a reduction in scale effects from the zero-damage level.

Table 1. Basic data.

Test designation <sup>1</sup>	$d/gT^2$	T	Armor layer thickness	$W_{50}$	$N_z$	$\bar{N}_{zp}$	b	$H_z$
		(s)	(cm)	(kg)				(cm)
SPL-17	0.0595	2.80	41.76	34.02	2.834	2.648	6.333	112.56
SPL-27	0.0595	2.80	29.56	12.25	2.462	2.648	5.151	69.56
SET-7	0.0588	0.89	5.12	0.034	1.870	-----	3.410	7.44
SET-8	0.0588	0.89	4.97	0.034	1.644	-----	2.210	6.52
SET-22	0.0588	0.89	4.97	0.034	2.267	-----	6.313	9.02
SET-24	0.0588	0.89	4.48	0.034	2.604	-----	5.694	10.33
SPL-18	0.0264	4.2	39.32	34.02	2.455	2.136	4.355	97.51
SPL-25	0.0264	4.2	52.43	34.02	2.185	2.136	5.969	86.78
SPL-28	0.0264	4.2	30.48	12.25	1.862	2.136	4.686	52.61
SPL-35	0.0264	4.2	55.47	54.43	2.042	2.136	3.736	94.85
SET-2	0.0264	1.33	5.40	0.034	1.816	-----	3.591	7.22
SET-4	0.0264	1.33	4.12	0.034	1.772	-----	3.902	7.04
SET-9	0.0264	1.33	5.03	0.034	1.610	-----	3.310	6.40
SET-19	0.0264	1.33	5.55	0.034	1.431	-----	2.844	5.67
SPL-19	0.0144	5.7	46.33	34.02	1.979	1.970	7.149	78.61
SPL-23	0.0144	5.7	44.81	34.02	1.803	1.970	5.179	71.60
SPL-29	0.0144	5.7	29.87	12.25	1.780	1.970	6.841	50.29
SPL-32	0.0144	5.7	42.37	54.43	2.359	1.970	8.206	109.58
SPL-36	0.0144	5.7	42.06	54.43	1.928	1.970	6.120	89.55
SET-1	0.0144	1.80	4.78	0.034	1.490	-----	3.512	5.88
SET-3	0.0144	1.80	4.51	0.034	1.412	-----	4.709	5.61
SET-10	0.0144	1.80	5.06	0.034	1.605	-----	5.682	6.37
SET-20	0.0144	1.80	4.82	0.034	1.624	-----	4.083	6.46
SPL-20	0.00646	8.5	43.89	34.02	2.051	2.059	7.614	81.47
SPL-24	0.00646	8.5	46.63	34.02	2.020	2.059	6.611	80.22
SPL-30	0.00646	8.5	25.91	12.25	2.165	2.059	12.195	61.17
SPL-33	0.00646	8.5	45.72	54.43	2.102	2.059	7.573	97.66
SPL-37	0.00646	8.5	51.51	54.43	1.959	2.059	5.396	91.01
SET-5	0.00646	2.69	4.45	0.034	1.406	-----	2.422	5.58
SET-6	0.00646	2.69	4.36	0.034	1.829	-----	5.040	7.13
SET-11	0.00646	2.69	4.48	0.034	1.805	-----	4.856	7.16
SET-21	0.00646	2.69	4.54	0.034	1.802	-----	4.705	7.16
SPL-22	0.00365	11.3	47.24	34.02	2.387	2.370	8.145	94.79
SPL-31	0.00365	11.3	29.26	12.25	2.235	2.370	6.687	63.15
SPL-34	0.00365	11.3	48.46	54.43	2.487	2.370	8.480	115.52
SET-12	0.00366	3.57	3.84	0.034	1.694	-----	7.000	6.64
SET-13	0.00366	3.57	4.18	0.034	1.649	-----	5.525	6.55
SET-23	0.00366	3.57	4.82	0.034	1.996	-----	8.479	7.92

<sup>1</sup>SPL: LWT test; SET: small-scale test.

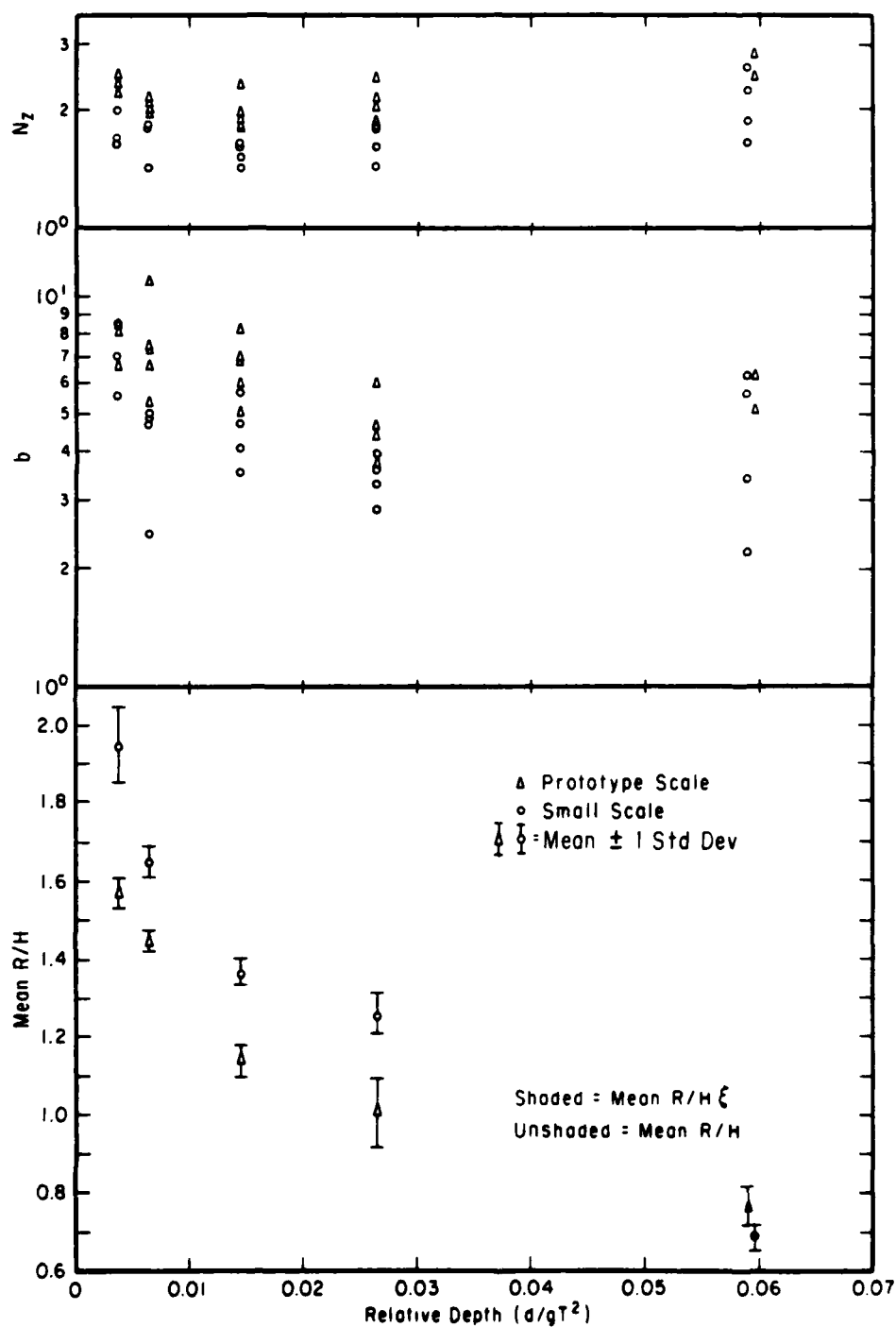


Figure 6. Zero-damage stability numbers, damage rate coefficients, and relative runup versus relative depth.

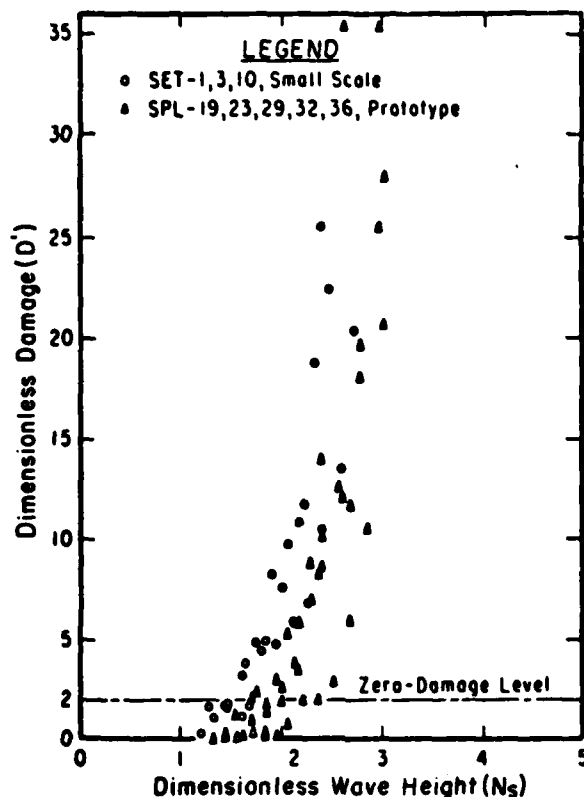


Figure 7. Small-scale and prototype damage trends for  $d/gT^2 = 0.0144$ .

In addition to the information on damage trends, Figure 6 shows that the small-scale tests exhibit less influence of wave period at the zero-damage level than the prototype tests. The prototype  $N_z$ 's have the characteristic parabolic trend of wave period that was observed in the data for slopes of 1 on 2.5 and 1 on 5, as discussed by Ahrens and McCartney (1975), while the small-scale  $N_z$ 's show a more linear trend.

## 2. Profile Shapes.

Another way to evaluate scale effects, particularly at high damage levels, is to compare the shapes of the damaged surface profiles for similar wave conditions. This comparison requires the use of data where the dimensionless damage is about the same at both small scale and prototype. Figure 8 shows a profile comparison for tests with short period waves ( $d/gT^2 = 0.0264$ ) and gives the dimensionless wave height and damage, respectively, for both tests in the legend. The profiles were made comparable by increasing the small-scale test dimensions by a factor of 10. The shapes of the two profiles were similar, and the causative dimensionless wave heights were about the same. Figure 9 is similar to Figure 8 except the profile comparison was for tests with long period waves ( $d/gT^2 = 0.0037$ ), and the causative dimensionless wave height was approximately 18 percent smaller in the small-scale tests.

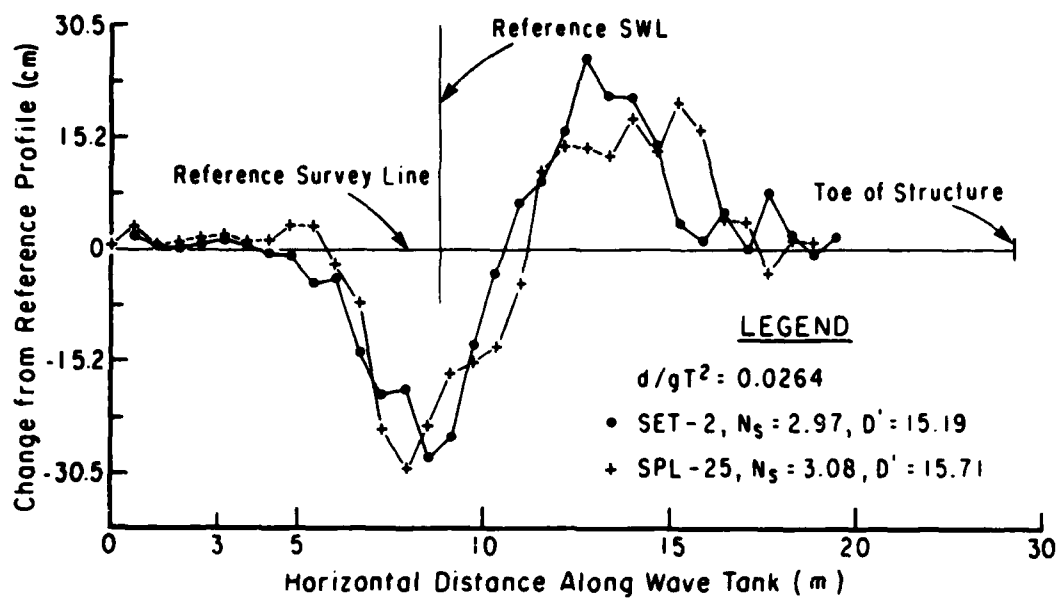


Figure 8. Small-scale and prototype damage profile comparison for  $d/gT^2 = 0.0264$ .

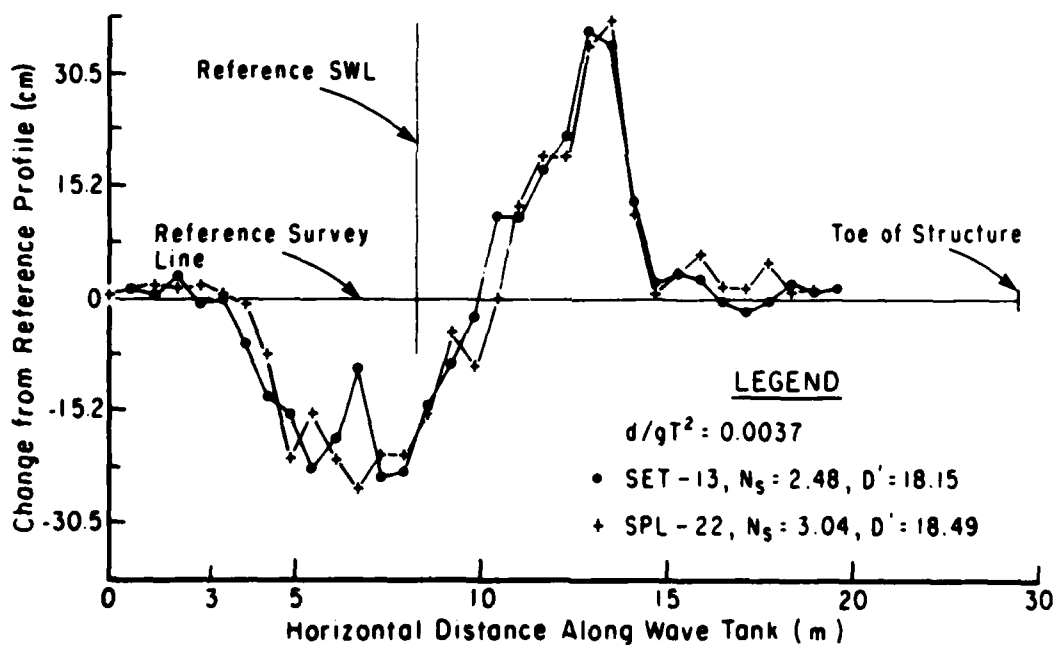


Figure 9. Small-scale and prototype damage profile comparison for  $d/gT^2 = 0.0037$ .



The correlation coefficients of the damage profiles provided a convenient means of comparing the damage profiles of the model and the prototype by calculating the coefficients for model and prototype tests with approximately the same relative damage. The profiles tests were matched by the location of the stillwater level on the reference surveys, and the averaged differences from the reference surveys for the model and prototype tests were paired to calculate the correlation coefficient. Table 2 provides a tabulation of correlation coefficients for a number of model-prototype profile pairs, including those shown in Figures 8 and 9. In general, the closer the relative depths of the model and prototype tests were the more similar the profile shapes.

### 3. Runup.

In evaluating scale effects between small-scale and large-scale tests the wave runup was also compared. Runup was visually defined as the average point of maximum wave uprush on the riprap surface near the center of the wave tank. The elevation of this point was then measured using the survey apparatus. The runup data in Table 3 indicate that relative runup,  $R/H$ , can be considered constant for a fixed value of  $d/gT^2$  between 0.0264 and 0.0036. For  $d/gT^2$  of 0.0595 or 0.0589, the ratio of the relative runup to the surf parameter,  $\xi$ , is almost constant, where the surf parameter,  $\xi$ , is defined as

$$\xi = (H/L_0)^{-1/2} \tan \theta,$$

$L_0$  is the deepwater wavelength, and  $\theta$  the angle between the embankment and the horizontal. The runup invariants,  $R/H$  or  $(R/H)/\xi$ , as tabulated in Table 3 and shown in Figure 6, indicate that the runup in the small-scale tests was approximately 20 percent greater than predicted from the prototype tests.

The small-scale test results at the zero-damage level give more conservative estimates of the stability number and the runup. The zero-damage level stability numbers are lower and the runup is higher in the small-scale tests than predicted by the prototype tests. The higher runup is probably due to the reduced penetration of the wave uprush in the small-scale tests as compared to the prototype tests. The stone size used in the filter layer was modeled geometrically but should be somewhat larger, according to Keulegan (1973), to obtain proper flow similitude.

### 4. Flow Regime.

In this study the small-scale tests replicated the prototype tests at a 1:10 Froude scale which, assuming no scale effects, required rough turbulent flow in both the small-scale and prototype-scale tests. When using the Froude scale model the model and prototype will be dynamically similar with respect to inertial and viscous forces because viscous forces can be assumed insignificant. The existence or nonexistence of rough turbulent flow is determined from the criterion established by Jonsson (1966). Using definitions similar to Madsen and White (1976), who applied Jonsson's criterion to rubble-mound structures, the Reynolds number,  $Re$ , is given by

$$Re = \frac{R_z^2 (1 + \cot^2 \theta) \left(\frac{2\pi}{T}\right)}{\nu} \quad (5)$$

Table 2. Correlation coefficients for model and prototype profiles.

Model	Prototype		
Test designation $d/gT^2$	SPL 25	SPL 19	SPL 22
	0.0264	0.0144	0.0037
SET-2 0.0264	0.847	0.927	0.796
SET-1 0.0144	0.848	0.899	0.752
SET-13 0.0037	0.607	0.702	0.946

Table 3. Runup.

Wave period, T (s)	$d/gT^2$	R/H		$\frac{R/H}{\xi}$		N	Std. dev. mean
		Mean	Std. dev.	Mean	Std. dev.		
2.89	0.0595	-----	-----	0.682	0.024	7	0.035
0.89	0.0588	-----	-----	0.760	0.051	18	0.067
4.20	0.0264	1.004	0.086	-----	-----	8	0.086
1.33	0.0264	1.257	0.050	-----	-----	4	0.040
5.7	0.0144	1.138	0.040	-----	-----	12	0.035
1.80	0.0144	1.366	0.033	-----	-----	5	0.024
8.5	0.0064	1.444	0.021	-----	-----	11	0.015
2.69	0.0064	1.649	0.040	-----	-----	6	0.024
11.3	0.0037	1.568	0.038	-----	-----	6	0.024
3.57	0.0037	1.948	0.097	-----	-----	13	0.050

and the roughness term,  $a_{im}/k$ , by

$$\frac{a_{im}}{k} = \frac{R_z (1 + \cot^2 \theta)^{1/2}}{\left( \frac{w_{50}}{w_r} \right)^{1/3}} \quad (6)$$

where  $R_z$  is the wave runup associated with the zero-damage wave height,  $H_z$ ;  $T$  the wave period; and  $\nu$  the kinematic viscosity. The values of runup used to compute the Reynolds number and roughness are tabulated by test in Table 4 and represent the estimated runup which would be caused by the zero-damage wave height. The estimates of  $R_z$  are calculated using the values of  $H_z$  in Table 1 with the runup invariants tabulated in Table 3. Since the Reynolds number defined in equation (5) uses wave runup, the calculations of the flow regime refer to surface conditions, not conditions in the filter layer. In Figure 10 the Reynolds number and roughness values tabulated in Table 4 are shown with the flow regime boundaries as updated by Jonsson (1978). The figure shows that both the small-scale and prototype tests are in the rough turbulent flow regime.

#### V. COMPARISON WITH OTHER SOURCES OF DATA

Scale effects at the zero-damage level were compared with the scale effects test results of Dai and Kamel (1969) and Thomsen, Wohlt, and Harrison (1972) in Figure 11; Dai and Kamel used rough quarrystone in their rubble-mound stability tests and Thomsen, Wohlt, and Harrison used dumped Kimmswick limestone in their riprap stability tests. The comparison was made by dividing the individual value of  $N_z$  by the average prototype value of  $N_z$  for the tests having the same relative depth (designated  $\bar{N}_{zp}$ ), as tabulated in Table 1 for this study, to form the scale effects factor  $N_z/\bar{N}_{zp}$ . Figure 11 shows the scale effects factor plotted versus a Reynolds number,  $R_N$ , which is given by

$$R_N = \frac{(gH_z)^{1/2} \left( \frac{w_{50}}{w_r} \right)^{1/3}}{\nu}$$

where  $H_z$  is the zero-damage wave height, and  $\nu$  the kinematic viscosity of water (assumed to be  $1.1306 \times 10^{-6}$  square meters per second corresponding to a water temperature of 15.6° Celsius). At the zero-damage level the stability numbers were approximately 20 percent lower for the small-scale test than for the prototype test, as shown in Figure 11. The figure also shows that at the zero-damage level the scale effects observed in this study were somewhat less severe than those observed by Thomsen, Wohlt, and Harrison and comparable to those observed by Dai and Kamel.

The small-scale test results of this study were also compared with a 1975 study conducted by the Hydraulic Research Station (HRS), Wallingford, England, for the Construction Industry Research and Information Association (CIRIA) (Hydraulic Research Station, 1975). The HRS study on riprap stability under irregular wave attack was conducted at small scale. Table 5 tabulates the HRS tests with a 1 on 4 or 1 on 3 slope which were used for comparison. These slopes

Table 4. Flow regime computations<sup>1</sup>.

Test designation	$d/gT^2$	T	$W_{50}$	$\nu$ $1 \times 10^{-5}$	$k$ <sup>2</sup>	$R_z$	$a_{im}/k$ (eq. 6)	$R_F$ $1 \times 10^{-5}$ (eq. 5)
SPL-17	0.0595	2.8	75	0.97	0.763	3.48	16.60	371
SET-22	0.0588	0.89	0.075	1.06	0.0763	0.313	14.94	8.65
SET-24	0.0588	0.89	0.075	1.02	0.0763	0.335	15.98	10.29
SPL-18	0.0264	4.2	75	0.92	0.763	3.21	15.32	222
SPL-25	0.0264	4.2	75	1.20	0.763	2.86	13.64	135
SET-2	0.0264	1.33	0.075	0.99	0.0763	0.300	14.33	5.71
SET-9	0.0264	1.33	0.075	1.00 <sup>3</sup>	0.0763	0.264	12.59	4.36
SET-19	0.0264	1.33	0.075	1.00 <sup>3</sup>	0.0763	0.234	11.15	3.42
SPL-19	0.0144	5.7	75	1.08	0.763	2.93	14.00	116
SPL-23	0.0144	5.7	75	1.50	0.763	2.67	12.75	63
SET-1	0.0144	1.80	0.075	1.00 <sup>3</sup>	0.0763	0.264	12.58	3.21
SET-3	0.0144	1.80	0.075	1.01	0.0763	0.251	11.93	2.89
SET-10	0.0144	1.80	0.075	1.00 <sup>3</sup>	0.0763	0.286	13.62	3.77
SET-20	0.0144	1.80	0.075	1.13	0.0763	0.291	13.82	3.43
SPL-20	0.00646	8.5	75	1.75	0.763	3.86	18.41	83
SPL-24	0.00646	8.5	75	1.48	0.763	3.80	18.13	96
SET-6	0.00646	2.69	0.075	1.06	0.0763	0.386	18.41	4.35
SET-11	0.00646	2.69	0.075	1.00 <sup>3</sup>	0.0763	0.388	18.49	4.65
SET-21	0.00646	2.69	0.075	1.12	0.0763	0.388	18.49	4.15
SPL-22	0.00365	11.3	75	1.59	0.763	4.87	23.26	110
SET-12	0.00366	3.57	0.075	1.00 <sup>3</sup>	0.0763	0.425	20.26	4.21
SET-13	0.00366	3.57	0.075	1.00 <sup>3</sup>	0.0763	0.419	19.98	4.09
SET-23	0.00366	3.57	0.075	1.03	0.0763	0.506	24.16	5.21

<sup>1</sup>All test  $\cot\theta = 3.5$ .<sup>2</sup> $k = (W_{50}/W_T)^{1/3}$ .<sup>3</sup>Assumed value of kinematic viscosity.

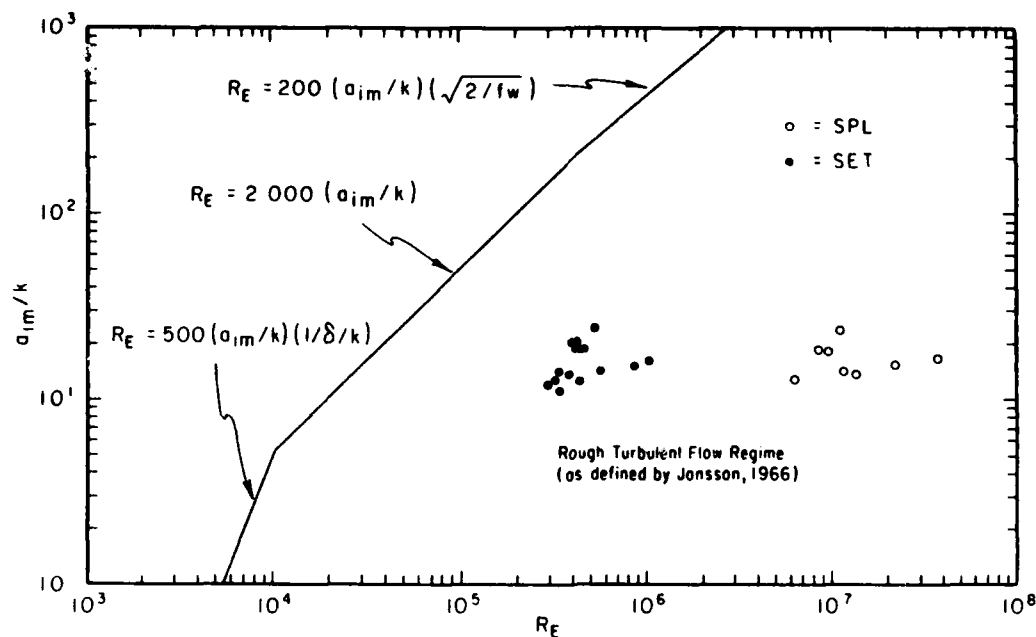


Figure 10. Flow regime.

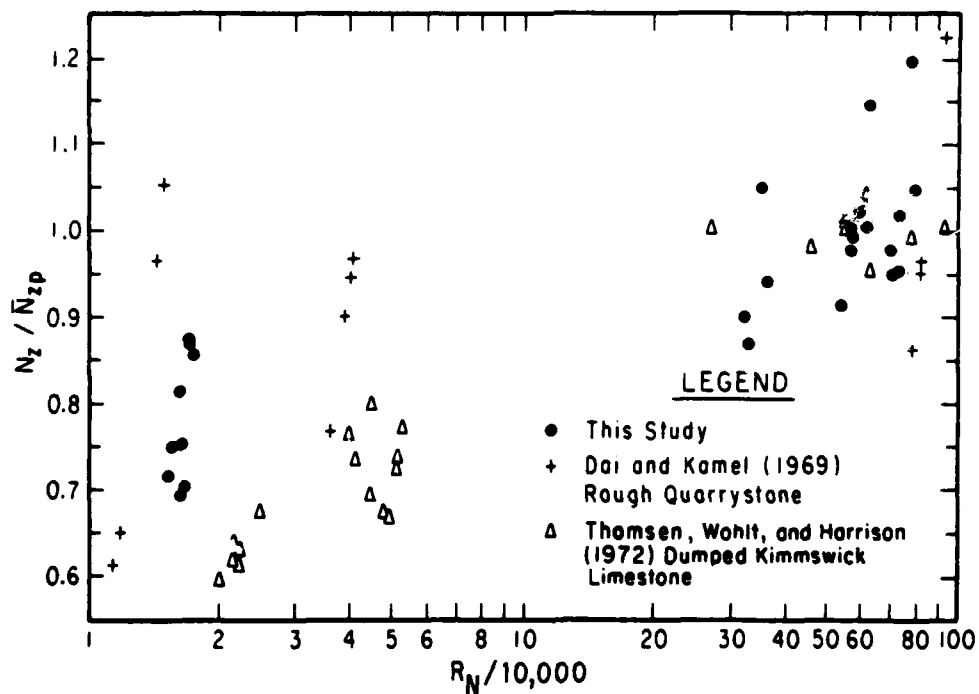


Figure 11. Scale effects factor versus Reynolds number for various sources of data.

Table 5. HRS data.

Tests	Slope	d (cm)	$D_{50}^R$	k	$N_z$ <sup>1</sup>	b <sup>1</sup>	$H_z$ <sup>2</sup> (cm)	$R_z$ <sup>3</sup> (cm)	$R_E$ <sup>4</sup> $1 \times 10^4$
49-61 <sup>5</sup>	1:3	61.0	2.0	1.64	1.1040	2.7063	3.08	4.23	72.9
108-112 <sup>6</sup>	1:3	30.5	2.0	1.64	1.4184	5.0614	3.95	5.98	209.2
33-46 <sup>5</sup>	1:3	61.0	3.0	2.46	1.2455	3.2222	5.21	8.49	29.4
113-116 <sup>7</sup>	1:3	46.1	3.0	2.46	1.4122	4.7379	5.91	9.88	460.9
62-67 <sup>5</sup>	1:3	61.0	4.0	3.28	1.3621	3.5014	7.50	13.26	71.8
117-127 <sup>5</sup>	1:4	61.0	2.0	1.64	1.6297	4.2240	4.54	5.41	203.5
166-169 <sup>6</sup>	1:4	30.5	2.0	1.64	1.7601	4.0394	4.91	5.87	342.8
128-140 <sup>5</sup>	1:4	61.0	3.0	2.46	1.6869	5.4265	7.05	8.55	507.7
170-173 <sup>8</sup>	1:4	61.0	4.0	3.28	1.6610	5.4753	9.26	11.31	888.0

<sup>1</sup>An equation of the form  $D' = aN_s^b$  was fitted to the data.

<sup>2</sup> $H_z$  predicted wave height at  $D' = 2.00$ .

<sup>3</sup> $R_z$  predicted runup for  $H_z$ .

<sup>4</sup> $R_E = \frac{R_z^2 (1 + \cot^2 \theta) (2\pi/T)}{v}$ , where  $v = 9.3 \times 10^{-3}$  square centimeters per second and  $d/gT^2 = 0.023$  is assumed.

<sup>5</sup> $T_p$  ranged from 1.66 to 1.15 seconds,  $d/gT^2$  ranged from 0.023 to 0.047.

<sup>6</sup> $T_p$  equaled 1.154 seconds,  $d/gT^2$  equaled 0.023.

<sup>7</sup> $T_p$  equaled 1.431,  $d/gT^2$  equaled 0.023.

<sup>8</sup> $T_p$  equaled 1.655,  $d/gT^2$  equaled 0.023.

were chosen because they bracketed the 1 on 3.5 slope used in the small-scale tests of this study. Only the small-scale tests with a relative depth of 0.0144 and 0.0264 were used. The relative depth of 0.0144 gave the lowest stability numbers and 0.0264 was in the range of relative depths tested in the HRS study. Figure 12 shows the stability numbers,  $N_z$ , versus the Reynolds number,  $Re$ , which is described by equation (5). From Figure 12 it can be hypothesized that riprap stability under irregular wave attack may be equivalent to the monochromatic tests with the relative depths that yield the lowest stability numbers.

## VI. RESULTS AND CONCLUSIONS

The results of this study showed a reduction of about 20 percent in the zero-damage stability numbers for a 1:10 (model:prototype) Froude scale model from the expected prototype values. The reduction of stability in the model appears to be related to the lack of penetration of the wave runup into the filter layer and the improper modeling of the flow regime within the filter layer. Figures 5 and 7 show that the difference between the small-scale tests and the prototype tests decreased as the damage level increased indicating that the scale effects decrease. The data points in Figure 7 indicate a convergence of the damage trends, whereas the equation  $D' = aN_z^b$ , as shown in Figure 5, shows a crossing of the damage trends. The convergence of damage trends seems reasonable because higher Reynolds numbers developed at higher damage level and the viscous forces became less significant. The crossing of the damage trends seems unreasonable and could be caused by the method used in deriving the equation  $D' = aN_z^b$ . The data points at the lower damage levels could be exerting more influence on the equation than is justified.

The following conclusions were reached:

1. The tests at a 1:10 (model:prototype) Froude scale yield zero-damage stability numbers about 20 percent lower than the prototype tests. This indicates that scale effects in this study were less severe than those found by Thomsen, Wohlt, and Harrison (1972).
2. Scale effects were less severe at high levels of damage than at the zero-damage level.
3. The runup at the zero level was about 20 percent higher in the small-scale tests than predicted by the prototype test.
4. The shapes of the damage profile for the small-scale and the prototype tests having the same relative depth were very similar.
5. At the zero-damage level, wave period had less influence in the small-scale tests than in the prototype tests.

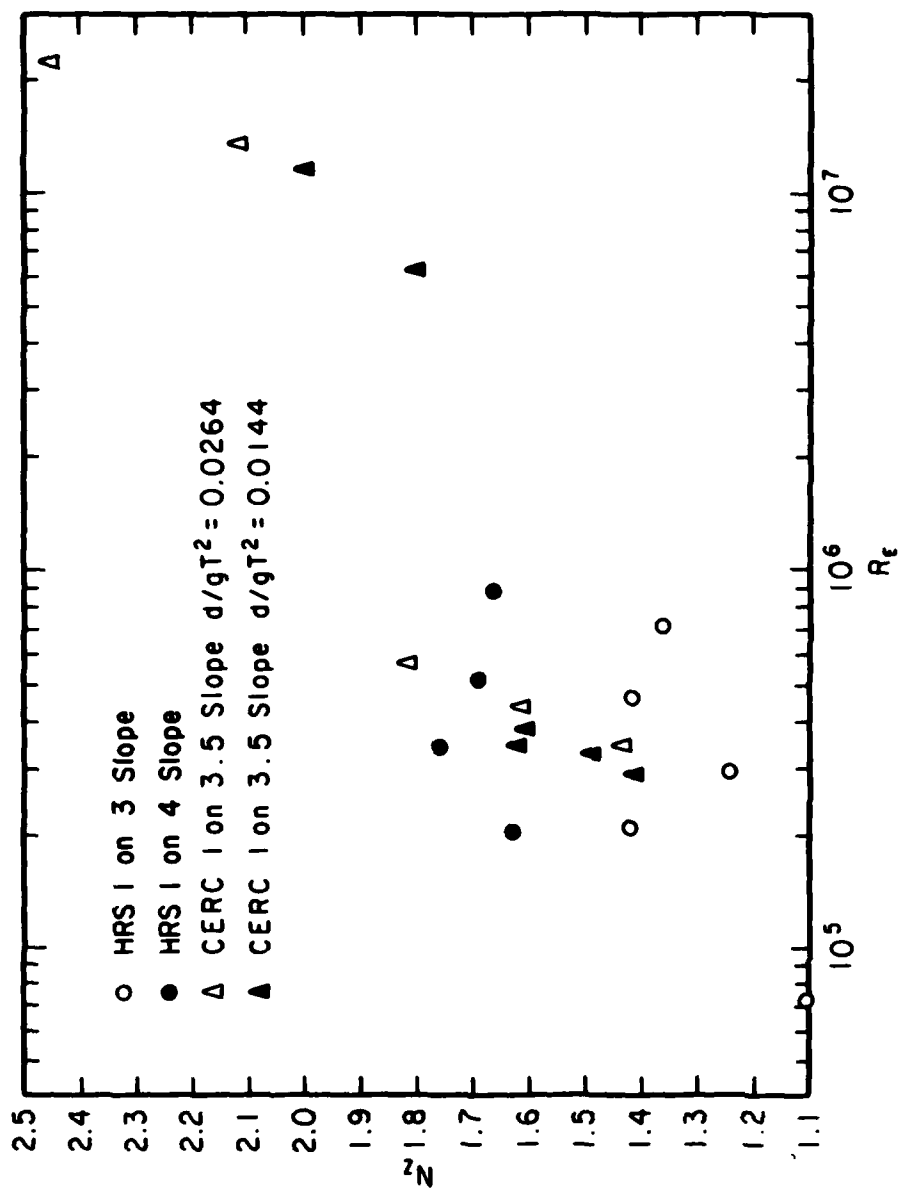


Figure 12. Stability numbers versus Reynolds numbers, HRS data.



#### LITERATURE CITED

- AHRENS, J.P., "Large Wave Tank Tests of Riprap Stability," TM 51, U.S. Army, Corps of Engineers, Coastal Engineering Research Center, Fort Belvoir, Va., May 1975.
- AHRENS, J.P., and McCARTNEY, B.L., "Wave Period Effect on the Stability of Riprap," *Proceedings of the Specialty Conference on Civil Engineering in the Oceans/III*, American Society of Civil Engineers, 1975 (also Reprint 76-2, U.S. Army, Corps of Engineers, Coastal Engineering Research Center, Fort Belvoir, Va., NTIS A029 726).
- COASTAL ENGINEERING RESEARCH CENTER, "Its Mission and Capabilities," U.S. Army Corps of Engineers, Fort Belvoir, Va., May 1980.
- DAI, Y.B., and KAMEL, A.M., "Scale Effect Tests for Rubble-Mound Breakwaters," Research Report H-69-2, U.S. Army Engineer Waterways Experiment Station, Vicksburg, Miss., 1969.
- HUDSON, R.Y., "Design of Quarry-Stone Cover Layers for Rubble-Mound Breakwaters; Hydraulic Laboratory Investigation," Research Report 2-2, U.S. Army Engineer Waterways Experiment Station, Vicksburg, Miss., 1958.
- HYDRAULIC RESEARCH STATION, "Riprap Design for Wind-Wave Attack, A Laboratory Study in Random Waves," Report No. EX 707, Wallingford, Oxfordshire, England, 1975.
- JONSSON, I.G., "Wave Boundary Layers and Friction Factors," *Proceedings of the 10th Conference on Coastal Engineering*, American Society of Civil Engineers, 1966.
- JONSSON, I.G., "A New Approach to Oscillatory Rough Turbulent Boundary Layers," Series Paper No. 17, Institute of Hydrodynamics and Hydraulic Engineering, Lyngby, Denmark, 1978.
- KEULEGAN, G.H., "Wave Transmission Through Rock Structures; Hydraulic Model Investigation," Research Report H-73-1, U.S. Army Engineer Waterways Experiment Station, Vicksburg, Miss., June 1973.
- MADSEN, O.S., "Waves Generated by a Piston-Type Wavemaker," *Proceedings of the 12th Conference on Coastal Engineering*, American Society of Civil Engineers, Vol. I, 1970, pp. 589-607 (also Reprint 4-71, U.S. Army, Corps of Engineers, Coastal Engineering Research Center, Fort Belvoir, Va., NTIS 732 607).
- MADSEN, O.S., and WHITE, S.M., "Reflection and Transmission Characteristics of Porous Rubble-Mound Breakwaters," MR 76-5, U.S. Army, Corps of Engineers, Coastal Engineering Research Center, Fort Belvoir, Va., Mar. 1976.
- THOMSEN, A.L., WOHLT, P.E., and HARRISON, A.S., "Riprap Stability on Earth Embankments Tested in Large- and Small-Scale Wave Tanks," TM 37, U.S. Army, Corps of Engineers, Coastal Engineering Research Center, Fort Belvoir, Va., June 1972.

<p>Broderick, Laurie L. Riprap stability scale effects / by Laurie L. Broderick and John P. Ahrens.--Fort Belvoir, Va. : U.S. Army, Corps of Engineers, Coastal Engineering Research Center; Springfield, Va. : available from NTIS, 1982.</p> <p>[29] p. : ill. ; 28 cm.--(Technical paper / Coastal Engineering Research Center ; no. 82-3) Cover title. "August 1982." "Literature Cited"; p. 29. Report provides an evaluation of small-scale tests of riprap stability at a 1:10 (model:prototype) Froude scale, which replicate previous tests of wave heights sometimes exceeding 5 feet conducted in the large wave tank at the Coastal Engineering Research Center.</p> <p>1. Riprap stability. 2. Scale effects--model studies. 3. Waves. I. Title. II. Ahrens, John P. III. Coastal Engineering Research Center (U.S.). IV. Series: Technical paper (Coastal Engineering Research Center (U.S.)) ; no. 82-3. TC203 .U581tp no. 82-3 627</p>	<p>Broderick, Laurie L. Riprap stability scale effects / by Laurie L. Broderick and John P. Ahrens.--Fort Belvoir, Va. : U.S. Army, Corps of Engineers, Coastal Engineering Research Center; Springfield, Va. : available from NTIS, 1982.</p> <p>[29] p. : ill. ; 28 cm.--(Technical paper / Coastal Engineering Research Center ; no. 82-3) Cover title. "August 1982." "Literature Cited"; p. 29. Report provides an evaluation of small-scale tests of riprap stability at a 1:10 (model:prototype) Froude scale, which replicate previous tests of wave heights sometimes exceeding 5 feet conducted in the large wave tank at the Coastal Engineering Research Center.</p> <p>1. Riprap stability. 2. Scale effects--model studies. 3. Waves. I. Title. II. Ahrens, John P. III. Coastal Engineering Research Center (U.S.). IV. Series: Technical paper (Coastal Engineering Research Center (U.S.)) ; no. 82-3. TC203 .U581tp no. 82-3 627</p>
<p>Broderick, Laurie L. Riprap stability scale effects / by Laurie L. Broderick and John P. Ahrens.--Fort Belvoir, Va. : U.S. Army, Corps of Engineers, Coastal Engineering Research Center; Springfield, Va. : available from NTIS, 1982.</p> <p>[29] p. : ill. ; 28 cm.--(Technical paper / Coastal Engineering Research Center ; no. 82-3) Cover title. "August 1982." "Literature Cited"; p. 29. Report provides an evaluation of small-scale tests of riprap stability at a 1:10 (model:prototype) Froude scale, which replicate previous tests of wave heights sometimes exceeding 5 feet conducted in the large wave tank at the Coastal Engineering Research Center.</p> <p>1. Riprap stability. 2. Scale effects--model studies. 3. Waves. I. Title. II. Ahrens, John P. III. Coastal Engineering Research Center (U.S.). IV. Series: Technical paper (Coastal Engineering Research Center (U.S.)) ; no. 82-3. TC203 .U581tp no. 82-3 627</p>	<p>Broderick, Laurie L. Riprap stability scale effects / by Laurie L. Broderick and John P. Ahrens.--Fort Belvoir, Va. : U.S. Army, Corps of Engineers, Coastal Engineering Research Center; Springfield, Va. : available from NTIS, 1982.</p> <p>[29] p. : ill. ; 28 cm.--(Technical paper / Coastal Engineering Research Center ; no. 82-3) Cover title. "August 1982." "Literature Cited"; p. 29. Report provides an evaluation of small-scale tests of riprap stability at a 1:10 (model:prototype) Froude scale, which replicate previous tests of wave heights sometimes exceeding 5 feet conducted in the large wave tank at the Coastal Engineering Research Center.</p> <p>1. Riprap stability. 2. Scale effects--model studies. 3. Waves. I. Title. II. Ahrens, John P. III. Coastal Engineering Research Center (U.S.). IV. Series: Technical paper (Coastal Engineering Research Center (U.S.)) ; no. 82-3. TC203 .U581tp no. 82-3 627</p>

D

FI

1

D